PHYSICAL REVIEW B **78**, 020101(R) (2008)

Phonon-confinement entropy and the formation of $CeH_{2.84}$ nanoplates by fracture

M. E. Manley,[1] F. Trouw,[2] D. Teter,[2] M. P. Hehlen,[2] P. A. Papin,[2] D. J. Thoma,[2] and W. L. Hults[2]
[1]*Lawrence Livermore National Laboratory, Livermore, California 94551, USA*
[2]*Los Alamos National Laboratory, Los Alamos, New Mexico 87545, USA*

(Received 29 February 2008; revised manuscript received 5 June 2008; published 31 July 2008)

Particles formed during the reaction of cerium with hydrogen fractured into stacked plates with fully separated plate thicknesses averaging 100 nm and a finer partially separated thickness of 30 nm. The phonon density of states of these particles, measured using inelastic neutron scattering, showed a low-energy feature that could not be accounted for in the phonon-dispersion curves of bulk crystals but was similar to a feature predicted for the confinement of phonons in nanoplates. The shift of modes to lower energies indicates that excess vibrational entropy is created by the fracture. We argue that this excess entropy contributes to the observed fracture pattern by introducing a characteristically weak size for fracture.

DOI: 10.1103/PhysRevB.78.020101 PACS number(s): 62.25.Mn, 63.22.Np, 78.70.Nx

Griffith's[1] criteria for the brittle fracture of a macroscopic solid are satisfied when the strain-energy release rate equals the energy of forming the fracture surfaces.[2] When the outcome of fracture is nanoplates, the phonon density of states (DOS) of the plates formed is different from that of the prefractured material and the associated free-energy changes must also be accounted for in the energy balance. While size effects on phonons are known to play a role in thermal transport, electronic processes, and thermodynamic stability,[3–13] little is known about their role in fracture. Nanostructures, however, typically exhibit low-energy enhancements of their phonon DOS,[5,12] increased vibrational amplitudes,[14–17] and, consequently, excess vibrational entropy.[5] Early theoretical work attributed the softer phonons to a volume relaxation, but this effect was limited to particles with dimensions of less than 5 nm.[18] More recent theoretical work shows that a 32.5 nm thick freestanding silicon plate exhibits pronounced changes in its phonon DOS from phonon confinement.[13] From the perspective of fracture this is a more significant prediction since the total amount of vibrational entropy per unit surface area increases with particle size. In this Rapid Communication we examine the phonon DOS of cerium hydride that, during the cerium-hydrogen reaction, fractured into stacked plates with fully separated plate thicknesses averaging 100 nm and a finer partially separated thickness of 30 nm.

Cerium hydride nanoplates were formed by reacting cerium and hydrogen in a closed evacuated system where hydrogen was released by heating uranium hydride to near 400 °C and reacted with cerium kept near room temperature. The uranium and cerium were kept thermally isolated by using a section of stainless-steel tubing. The process was partially reversed by heating cerium to 350 °C and cooling uranium. It was found that three cycles were needed to ensure that all cerium had reacted. The final cerium hydride product was partially reduced to a composition of $CeH_{2.84}$, as determined by lattice parameters[19] measured by x-ray diffraction. The material was transferred within the same closed system to a flat aluminum pan appropriate for neutron scattering. Neutron spectra were obtained on the LANSCE-PHAROS time-of-flight chopper spectrometer at Los Alamos National Laboratory. The incident neutron energy was 25 meV. The raw data were corrected for sample environment background, detector efficiency, and the k_i/k_f phase-space factor. Material was also removed in an argon filled glovebox and placed in containers for x-ray diffraction and scanning electron microscopy (SEM). Samples left open in the glovebox or left sealed under Kapton films formed ceria in a matter of days, as observed by diffraction. When ceria formed this way, however, it retained the nanostructure discussed below.

Figures 1(a) and 1(b) show the first set of SEM images taken as the formed cerium hydride powder. They show a stacked plate nanostructure with plate thicknesses averaging around 100 nm with only a few at 30 nm. Size broadening in the x-ray diffraction pattern, however, indicated that the average was closer to 30 nm. This discrepancy was resolved by

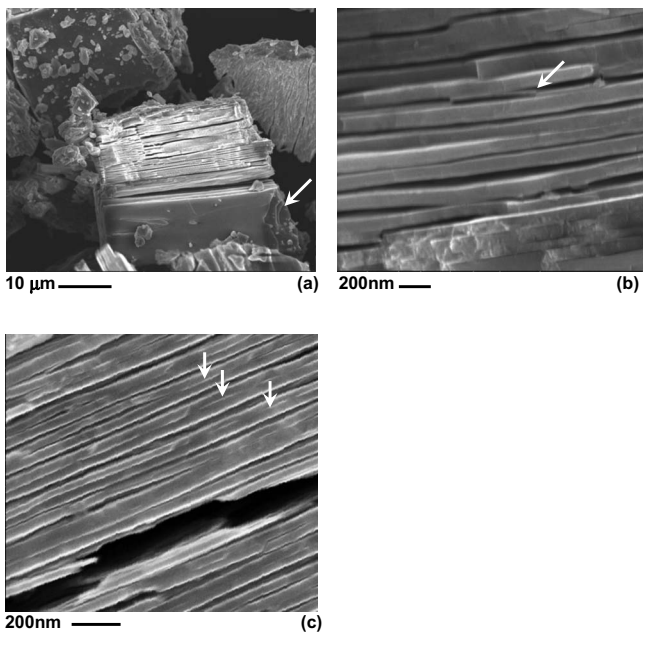

FIG. 1. Scanning electron microscope images of cerium hydride stacked-plate nanostructure. (a) Typical stacked-plate cluster. Arrow indicates region where plate layers can be distinguished from above. (b) Close-up view of the edges of the plates in (a). Arrow indicates a 30 nm thick plate. (c) Close-up view of another particle showing a finer fracture scale indicated by arrows.

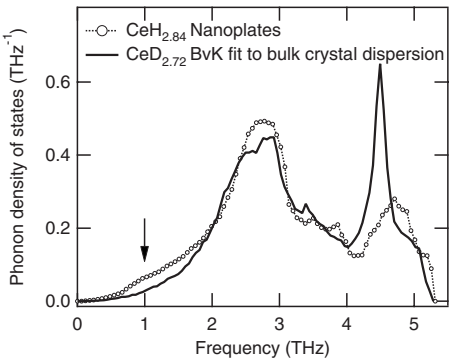

FIG. 2. Phonon DOS of cerium hydride determined by inelastic neutron scattering. The solid line was calculated from a force-constant model fit to dispersion curves measured on a bulk crystal with a similar composition by Vorderwisch *et al.* (Ref. 13). The data points were extracted from an incoherent measurement on the nanoplates (see text).

a second set of SEM images taken at a tilt [Fig. 1(c)]. In these images smaller incomplete fracture lines were observed, explaining the 30 nm scale implied by the x-ray diffraction results. Evidently, the hydride processes produce both complete and partial fractures along planes spaced at 100 and 30 nm, respectively. The fine scale fracture likely results from a combination of factors, including a slow bulk diffusion rate for hydrogen in cerium,[20] a large transformation volume change,[19] a brittle hydride,[21] as well as effects from phonon confinement, as will be discussed below.

Neutron scattering from these samples was dominated by incoherent scattering from hydrogen, which has a cross section nearly 40 times that of cerium and is nearly three times as abundant. However, in the low-energy range measured here, the dynamics are dominated by the motion of the cerium atoms; the hydrogen are simply carried along.[22] In this case, the phonon DOS at thermal energies can be extracted from the measured incoherent scattering. The procedure, described in detail elsewhere,[23] involves subtracting the multiphonon scattering determined iteratively to all orders, correcting for the Debye-Waller factor, and dividing out the thermal occupation factor. To improve statistics the data were summed over the high angle detector banks, where the phonon scattering is most intense.

The resulting phonon DOS, shown in Fig. 2, is compared with the phonon DOS of $CeD_{2.72}$ calculated using the Born von Karman model fit to single-crystal phonon-dispersion data by Vorderwisch *et al.*[22] While many of the differences might be attributed to the composition difference and instrument resolution, the 1 THz peak in the nanoplate phonon DOS (Fig. 2) cannot be explained this way. No phonon branches dip even close to this energy.[22] Cerium metal was also measured but the lowest-energy peak from its phonon DOS was well above the 1 THz feature, ruling out unreacted cerium metal as an explanation. Unreacted hydrogen is also unlikely since the sample holder was evacuated and the material was partially reduced, so any remaining hydrogen should have reacted. The reproducibility of the intensity of the 1 THz feature with subsequent measurements on different samples also supports these conclusions since the amount of residual reactance would be expected to vary somewhat from sample to sample. These observations leave the stacked-plate nanostructure itself as the most likely explanation for the 1 THz feature. This conclusion is further supported by the calculations of Hepplestone and Srivastava[13] showing that as silicon plates are thinned to near 30 nm extra peaks appear in the phonon DOS, including a peak in the low-energy acoustic range.[13]

The appearance of the low-energy feature in the phonon DOS indicates that excess entropy, $\Delta S_{\mathrm{vib}}^{\mathrm{ex}}$, is generated by the fracture.[5] Therefore, under isothermal conditions, the fracture into nanoplates is accompanied by the absorption of heat, $T\Delta S_{\mathrm{vib}}^{\mathrm{ex}}$, and a corresponding entropic force favoring the fracture. This force, caused by the thermal excitation of the formed low-energy phonons, is analogous to the configurational-entropic forces described in biological and colloidal interactions.[24] The time scale for phonon excitations is typically of order picoseconds, while crack growth is a slower process involving the simultaneous displacement of many planes of atoms over a relatively large distance compared to atomic vibrations. Thus, the confinement of phonons should occur instantaneously as the crack propagates. For a single separated layer the corresponding free-energy change from phonon confinement (per unit area) is given by

$$\Delta F_{\mathrm{conf}} = -t\rho T\Delta S_{\mathrm{vib}}^{\mathrm{ex}}, \tag{1}$$

where t is the layer thickness, ρ is the number of atoms per unit volume, and $\Delta S_{\mathrm{vib}}^{\mathrm{ex}}$ is the change in vibrational entropy per atom from phonon confinement. Assuming that the phonon states in the low-energy peak are distributed uniformly over the phonon DOS before confinement, the vibrational entropy generated is $\Delta S_{\mathrm{vib}}^{\mathrm{ex}} \approx 0.1\ k_B/(\text{cerium atom})$ at $T=300$ K, a value comparable to entropies found for other nanostructures.[5] Accounting for ρ and setting $t=30$ nm, Eq. (1) gives $\Delta F_{\mathrm{conf}} \approx -0.3\ \mathrm{J/m^2}$ at 300 K. The energy required to make a pair of surfaces in a pure metal ranges from about $2\gamma_s = 0.8\ \mathrm{J/m^2}$ for zinc to about $2\gamma_s = 3.8\ \mathrm{J/m^2}$ for iron,[25] but the presence of hydrogen significantly reduces fracture energies.[2] The surface energy of iron is reduced to $2\gamma_s = 0.91\ \mathrm{J/m^2}$ and that of aluminum is reduced from $2\gamma_s = 2.30$ to $2\gamma_s = 0.76\ \mathrm{J/m^2}$ in the presence of hydrogen.[26] While a value for the fracture energy of cerium hydride has not been reported, noted difficulties with the brittleness of rare crystals indicate that it must be very low.[21] Hence a phonon confinement free-energy change in order of $-0.3\ \mathrm{J/m^2}$ cannot be neglected.

Perhaps even more interesting than the energetically significant magnitude of the phonon-confinement free energy is its thickness dependence. While the frequencies vary in complicated ways with thickness, analysis of specific phonons indicates that they scale as powers of the thickness, $\omega_j(t) = A_j/t^{\alpha_j}$, where A and α are constants.[27] Assuming that the relevant phonons behave this way, the classical ($k_BT > \hbar\omega$) vibrational entropy change as a function of thickness is

$$\Delta S_{\mathrm{vib}}^{\mathrm{ex}}(t) \cong -3k_B \sum_j \ln[\omega_j(t)/\omega_j^{\mathrm{bulk}}] \approx 3k_B \sum_j \alpha_j \ln(C_j t), \tag{2}$$

where the $C_j = (A_j/\omega_j^{\mathrm{bulk}})^{1/\alpha_j}$ are constants. The important point is that the entropy terms scale logarithmically. Remov-

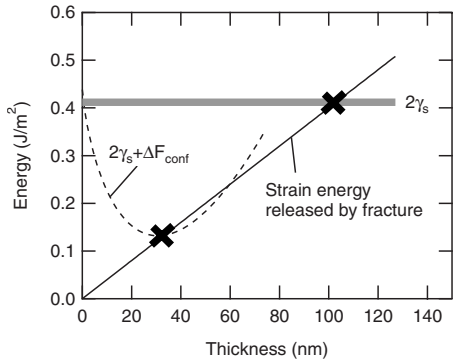

FIG. 3. Approximate fracture energy diagram with a phonon confinement effect superimposed at low plate thicknesses. The gray line indicates the energy required to form a pair of surfaces in the bulk, $2\gamma_s$. The dashed line indicates a proposed correction to the energy requirement owing to phonon confinement (see text). The solid black line indicates the potential strain energy to be released by fracture as a function of hydride layer thickness. The mark ***x*** indicate thicknesses where fracture could initiate.

ing the j's by assuming average values for the constants, the free energy [Eq. (1)] has the form

$$\Delta F_{\mathrm{conf}}(t) \cong -t(\rho 3k_B\alpha)\ln(Ct) = -tB\,\ln(Ct). \qquad (3)$$

This expression exhibits at minimum at $t_{\min}=1/eC$, indicating a characteristically weak thickness for fracture. This minimum comes about because of a competition between an increasing confinement effect per atom (logarithmic term) and a decreasing number of atoms in the layer (linear term) with decreasing thickness. Setting $t_{\min}=30$ nm (observed minimum thickness) and ΔF_{conf} (30 nm)$=-0.3$ J/m^2 (estimate from phonon DOS) yields $C=0.012$ nm^{-1} and $B=-0.01$ J/m^2 nm^{-1}. Superimposing Eq. (3) with these values on a conventional energy diagram for fracture (Fig. 3) suggests a possible explanation for the observed fracture pattern. First, as the hydride layer thickens during the hydride process the potential strain energy released by fracture increases linearly, solid black line. In the standard picture fracture occurs when the strain-energy released exceeds the energy cost of forming the new surfaces, $2\gamma_s$, upper mark at 100 nm in Fig. 3 (taken to be 0.41 J/m^2 for the sake of argument). Adding the confinement effect, however, introduces a narrow thickness range where the energy required to create the layers is reduced. Fracture can occur in this range, lower mark near 30 nm in Fig. 3, but only if the crack propagates along a path that maintains the special thickness. This thickness constraint would inhibit crack growth in the presence of nonuniform hydride transformation front or intrinsic impediments to crack growth. Hence, complete fracture is not expected until the layers reach 100 nm. Consequently a pattern of partial fracture near 30 nm and complete fracture at 100 nm is anticipated, consistent with observations (Fig. 1).

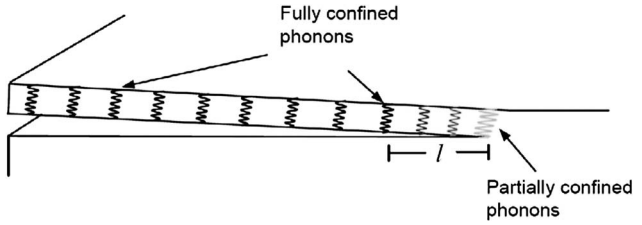

FIG. 4. Detailed nanoscale fracture process including phonon confinement. Near the crack tip the phonons are only partially confined. The distance from the crack tip to where the phonons are fully confined is defined as l.

In the present analysis, the correction to the fracture energy is determined from the final state of phonon confinement. During the fracture process, however, the phonons near the crack tip are not fully confined (see Fig. 4). This is not a problem for a long crack, since each increment of crack growth is accompanied by a corresponding increment of fully confined phonons further up in the free layer. However, for cracks shorter than a characteristic length l in Fig. 4, the situation is more complicated since the degree of confinement will depend on crack length.

While more work is needed to confirm the details of this nanoscale fracture process, the weak size effect is general and should be at least as important as the phonon-confinement stabilization of nanostructures.[12] Unlike with thermodynamic stability, fracture is a weak-link process, meaning that even a local weakening could be important in dictating the fracture process. This could have important consequences not only for small materials but also for the way cracks propagate in nanostructured bulk materials.

M.E.M. acknowledges useful discussions with Mark Asta. This work was performed under the auspices of the U.S. Department of Energy by Lawrence Livermore National Laboratory under Contract No. DE-AC52–07NA27344.

[1] A. A. Griffith, Philos. Trans. R. Soc. London **A221**, 163 (1920).
[2] T. L. Anderson, *Fracture Mechanics: Fundamentals and Applications*, 3rd ed. (CRC, Boca Raton, FL, 2005).
[3] A. Tanaka, S. Onari, and T. Arai, Phys. Rev. B **47**, 1237 (1993).
[4] M. Fujii, Y. Kanzawa, S. Hayashi, and K. Yamamoto, Phys. Rev. B **54**, R8373 (1996).
[5] B. Fultz, C. C. Ahn, E. E. Alp, W. Sturhahn, and T. S. Toellner, Phys. Rev. Lett. **79**, 937 (1997).
[6] J. Zou and A. Balandin, J. Appl. Phys. **89**, 2932 (2001).
[7] M. A. Stroscio and M. Dutta, *Phonons in Nanostructures* (Cambridge University Press, Cambridge, England, 2001).
[8] M. Seong, O. Mićić, A. Nozik, A. Mascarenhas, and H. Cheong, Appl. Phys. Lett. **82**, 185 (2003).
[9] A. P. Mayer, D. Bonart, and D. Strauch, J. Phys.: Condens. Matter **16**, S395 (2004).
[10] A. F. Yue, A. Papandrew, O. Delaire, B. Fultz, Z. Chowdhuri, R. M. Dimeo, and D. A. Neumann, Phys. Rev. Lett. **93**, 205501 (2004).

[11] A. A. Balandin, J. Nanosci. Nanotechnol. **5**, 1015 (2005).
[12] A. Kara and T. S. Rahman, Surf. Sci. Rep. **56**, 159 (2005).
[13] S. P. Hepplestone and G. P. Srivastava, Appl. Phys. Lett. **87**, 231906 (2005).
[14] G. von Eynatten, J. Horst, K. Dransfeld, and H. E. Bommel, Hyperfine Interact. **29**, 1311 (1986).
[15] M. Hayashi, E. Gerkema, A. M. van der Kraan, and I. Tamura, Phys. Rev. B **42**, 9771 (1990).
[16] H. Kuwano, H. Ouyang, and B. Fultz, Nanostruct. Mater. **1**, 143 (1992).
[17] L. B. Hong, C. C. Ahn, and B. Fultz, J. Mater. Res. **10**, 2408 (1995).
[18] M. Hasegawa, K. Hoshino, and M. Watabe, J. Phys. F: Met. Phys. **10**, 619 (1980).
[19] W. L. Korst and J. C. Warf, Inorg. Chem. **5**, 1719 (1966).
[20] D. Sraussi, I. Jacob, J. Bloch, N. Shamir, and M. H. Mintz, J. Alloys Compd. **191**, 91 (1993).
[21] G. G. Libowitz and J. G. Pack, J. Phys. Chem. Solids Suppl. **2**, 129 (1967).
[22] P. Vorderwisch, S. Hautecler, and W. Wegener, J. Less-Common Met. **74**, 117 (1980).
[23] M. E. Manley, R. J. McQueeney, B. Fultz, R. Osborn, G. H. Kwei, and P. D. Bogdanoff, Phys. Rev. B **65**, 144111 (2002).
[24] J. Israelachvili and H. Wennerström, Nature (London) **379**, 219 (1996).
[25] *Handbook of Physical Quantities*, edited by I. S. Grigoriev and E. Z. Meilikov (CRC, New York, 1997), p. 417.
[26] D. E. Jiang and E. A. Carter, Acta Mater. **52**, 4801 (2004).
[27] S. P. Hepplestone and G. P. Srivastava, Nanotechnology **17**, 3288 (2006).